

Weak stochastic ratchets and dynamic localization in measurement-induced quantum trajectories

I. Babushkin

*Institute of Quantum Optics, Leibniz University Hannover, Welfengarten 1, 30167 Hannover, Germany and
Max Born Institute, Max-Born-Strasse 2a, 10117, Berlin, Germany*

(Dated: March 1, 2022)

We consider a qubit governed by a sequence of weak measurements, with the measurement strength modified in a time- and state-dependent manner. The resulting trajectory of the qubit in the phase space can be weakly controlled without any direct action on the qubit (control-free control), even only one fixed observable is measured. Here we show a possibility of a weak form of a stochastic ratchet, allowing to create an additional “force” without changing the corresponding effective average potential. Furthermore, if the weak measurement strength is significantly reduced in a way conditioned to some particular state, a dynamical localization near this state takes place. If the measurement strength is reduced to zero, a singularity appears, which behaves like an artificial basis state.

PACS numbers: 42.50.Dv, 05.40.Fb, 03.65.Xp, 05.40.Jc

I. INTRODUCTION

Dynamics of quantum systems with the states frequently monitored by a measurement apparatus can be rather controversial and is a subject of constant interest over the years [1–15]. Every measurement in the measurement sequence may be tuned to cause only a partial collapse of the system’s wave function, with the collapse effect being arbitrary weak (so called “weak measurements”) [4, 8, 16–18]. In another context, the term “weak measurement” was introduced by Aharonov, Albert, and Vaidman (AAV) [19] as being attributed to a measurement of a continuous degree of freedom (e. g. an electron position) coupled to a discrete one (spin) via post-selection. These two approaches were recently shown to be equivalent [20, 21]. As a result of repetitive application of weak measurements — the situation which is sometimes referred to as weak Zeno measurements (WZM) — a kind of stochastic “quantum trajectory” arises [3, 14, 22–24] due to unpredictable character of every particular measurement outcome.

Just repeating the weak measurements, without any further action on the system, allows to control the system state in various ways. For instance, one can achieve an arbitrary state from any other one by repeating weak measurements in different bases [2, 5, 6, 12, 13, 25, 26]. Alternatively, by allowing the strength of the weak measurements (in AAV sense) to depend on the spatial coordinate, one can create a “potential wall” which may reflect a particle [12, 13]. It should be noted that these control mechanisms work if the initial state is pre-known.

In contrast, if we repeat a weak measurement of a single qubit in a fixed basis, the resulting dynamics was up to now believed to be very trivial. The resulting quantum trajectory just stochastically approaches one of the two qubit’s basis states $|0\rangle$ or $|1\rangle$. In this article we add a new dimension to this seemingly trivial dynamics by allowing the measurement strength to be changed in time and in a state-conditional way.

We observe that the stochastic equations, describing quantum trajectories in such simple one-dimensional system are in fact quite similar to the ones describing motion of a small Brownian particle in a fluid flow (overdamped Brownian motion) [23, 27–29]. One of the striking phenomena in such flows as well as in many other stochastic systems are so called stochastic ratchets. Namely, by varying the potential acting on the Brownian particle in time and/or space in a periodic way, it is possible to create an effective additional force, despite the potential introduces no average force [27–29]. Such ratchets are encountered in many stochastic systems of different nature [27–33]. Brownian ratchets are deeply connected to so called Parrondo games, when two or more lossy games are combined to give a winning one [30, 34, 35]. Very recently, the notion of weak Parrondo games and weak Brownian ratchets were introduced in [30] to describe the situation when two or more lossy games are played together to give just less lossy (but not winning) one. We remark that, although both Parrondo games and Brownian ratchets were considered in context of quantum systems [28, 36–39], this was up to now done via some direct action on the system itself.

In contrast, in the present article the situation of control-without-direct-action will be discussed. Here we show how the effective potential arising in WZM dynamics can be modified by changing the strength of the measurement periodically in time and in a state-conditioned fashion (that is, in dependence on the current system state). We demonstrate that the stochastic ratchet effect, albeit weak, is possible in such situation. We also demonstrate a dynamic localization of the state in the case when the measurement strength vanishes at some particular system state. A “false basis state” may appear, which “attracts” the stochastic trajectories in similar way as the true basis states do.

The article is organized as follows: in Sec. II we introduce the system under consideration and derive the master equation governing the probability distribution

on the line between two basis states; In Sec. III we derive the equation for the continuous case taking into account conditionally-dependent measurement strength; In Secs. IV-V we investigate the effects related to the conditionally modified measurements strength. Finally, the conclusions and discussion are presented in Sec. VI.

II. DISCRETE DYNAMICS

A. The setting

Our model of weak Zeno measurements is depicted in Fig. 1(a) and uses projective measurements of ancilla qubit $|a\rangle$ to realize the weak ones of $|q\rangle$. The system is prepared in the state $|q\rangle \otimes |0\rangle$ with $|q\rangle = \cos\theta |0\rangle + \sin\theta |1\rangle$ for some θ . First, we apply a rotation $R_y(2\delta)$ to the ancilla state; the rotation R_y is conditioned to $|q\rangle = |1\rangle$ and is defined as:

$$\begin{aligned} R_y(\delta) |0\rangle &\mapsto \cos\delta |0\rangle + \sin\delta |1\rangle, \\ R_y(\delta) |1\rangle &\mapsto \cos\delta |1\rangle - \sin\delta |0\rangle. \end{aligned} \quad (1)$$

Afterwards, we unconditionally apply the rotation R_y by some other angle α and finally we measure the ancilla qubit. If $\alpha \neq 0$ and δ is small, the resulting measurement modifies $|q\rangle$ only slightly. After the measurement, we repeat the whole procedure using another ancilla in the initial state $|0\rangle$ (or the same ancilla returned to the state $|0\rangle$).

The state of the whole system $|q\rangle \otimes |0\rangle$ [see Fig. 1(a)] is transformed by two R_y operators described above as:

$$|q\rangle \otimes |0\rangle \mapsto |q_0\rangle \otimes |0\rangle + |q_1\rangle \otimes |1\rangle, \quad (3)$$

$$|q_i\rangle = \sum_j b_{ij} |j\rangle, \quad (4)$$

where b_{ij} are $(i+1, j+1)$ th element of the matrix b defined as:

$$b = \begin{pmatrix} \cos\theta \cos\alpha & \sin\theta \cos(\delta + \alpha) \\ \cos\theta \sin\alpha & \sin\theta \sin(\delta + \alpha) \end{pmatrix}. \quad (5)$$

If the measurement of $|a\rangle$ gives 0, the system state is reduced to $|q\rangle = |q_0\rangle / \sqrt{p_0}$ and in the opposite case to $|q\rangle = |q_1\rangle / \sqrt{p_1}$, where

$$p_0 = \cos^2\alpha \cos^2\theta + \sin^2\theta \cos^2(\delta + \alpha), \quad (6)$$

$$p_1 = \cos^2\theta \sin^2\alpha + \sin^2\theta \sin^2(\delta + \alpha). \quad (7)$$

The probabilities of the corresponding outcomes are p_0 and p_1 .

The above description can be reformulated in the form of a generalized measurement formalism, with the measurement operators

$$\mathcal{B}_0 = b_{11} |0\rangle \langle 0| + b_{12} |1\rangle \langle 1|, \quad (8)$$

$$\mathcal{B}_1 = b_{21} |0\rangle \langle 0| + b_{22} |1\rangle \langle 1|, \quad (9)$$

so that $\sum_j \mathcal{B}_j^\dagger \mathcal{B}_j = 1$ and the state after the measurement with the result j is transformed as: $|q\rangle \rightarrow \mathcal{B}_j |q\rangle / \sqrt{p_j}$.

The resulting process is a (classical) one-dimensional random walk along the axis θ as shown in Fig. 1(b). It spends most of time in the vicinity of the limiting states $|q\rangle = |0\rangle$ and $|q\rangle = |1\rangle$ ($\theta = 0, \pi/2$). It is thus useful to introduce parabolic coordinates [17] as:

$$x = \operatorname{atanh}\{-\cos(2\theta)\}; \quad \theta = \arcsin \sqrt{\frac{1 + \tanh x}{2}}. \quad (10)$$

In this coordinate system, $\theta = 0$ corresponds to $x = -\infty$ and $\theta = \pi/2$ corresponds to $x = +\infty$ [(cf. Fig. 1(b)). Using x instead of θ allows to expand these vicinities into semi-infinite intervals. We also note that if we measure $|q\rangle$ directly (instead of $|a\rangle$), the probability to find $|q\rangle$ in the state $|1\rangle$ will be:

$$\Pi(x) = \sin^2\theta = (1 + \tanh x)/2. \quad (11)$$

B. Classical random walk interpretation

Now, for the sake of simplicity, we exclude the situation when $|q\rangle$ is exactly in one of the basis states $|0\rangle$ or $|1\rangle$ in the beginning of the process. In this case, the equations above allow to define the process as a one-dimensional random walk on the line $x \in (-\infty, +\infty)$ in the following way: assuming that at the n th iteration step the system is in the point x_n , at the $n+1$ step it will be in the point either $x_{n+1} = x_n + \epsilon_0$ or $x_{n+1} = x_n + \epsilon_1$ (depending on the measurement outcome), every of two variants occurring with the probabilities $p_i(x_n)$, $i = 0, 1$. Few realizations of this random walks are shown in Fig. 1(b).

The probabilities $p_i(x)$ can be rewritten in x -coordinates as:

$$p_0(x) = \Pi(x) \cos^2(\delta + \alpha) + (1 - \Pi(x)) \cos^2\alpha, \quad (12)$$

$$p_1(x) = \Pi(x) \sin^2(\delta + \alpha) + (1 - \Pi(x)) \sin^2\alpha, \quad (13)$$

where $\Pi(x)$ is defined by Eq. (11). The step sizes ϵ_i , $i = 0, 1$, do not depend on x and are given by (see details in A):

$$\epsilon_0 = \operatorname{atanh}\left(\frac{2 \cos^2(\alpha + \delta)}{\cos^2(\delta + \alpha) + \cos^2\alpha} - 1\right), \quad (14)$$

$$\epsilon_1 = \operatorname{atanh}\left(\frac{2 \sin^2(\alpha + \delta)}{\sin^2(\delta + \alpha) + \sin^2\alpha} - 1\right). \quad (15)$$

Eqs. (12)-(15) define obviously a Markovian random walk.

C. Conditionally varied measurement parameters

Suppose, we know exactly the initial state of the system x_0 and are able to make all the rotations also exactly.

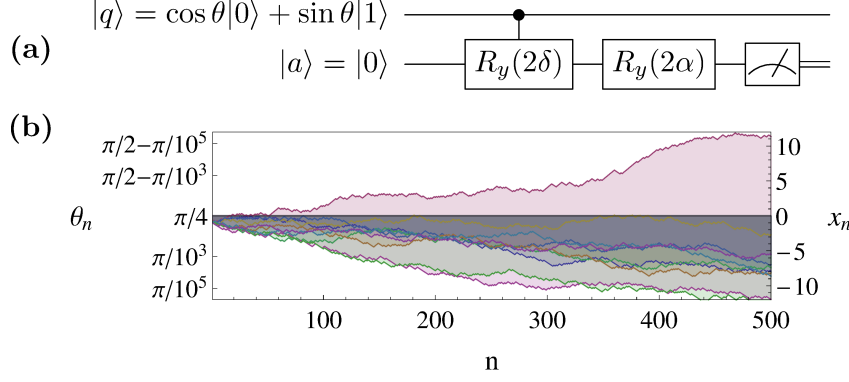


FIG. 1. (a) The model of weak measurements of the qubit $|q\rangle$ using an ancilla $|a\rangle$ (initially in the state $|0\rangle$) and its rotations R_y , followed by the measurement of $|a\rangle$. After the measurement, the process is repeated with the same or another ancilla in the state $|0\rangle$. In (b), the stochastic process induced by repeating application of (a) using θ coordinates (left y-axis) and x -coordinates given by Eq. (10) (right y-axis) vs. measurement number n is shown. The x -coordinates are obviously better suitable to study the asymptotic behavior as $n \rightarrow \infty$.

In this case, the subsequent positions x_n of the qubit on x -line can be also calculated exactly since we know the measurement outcomes $M_n = 0, 1$ and thus the step sizes ϵ_i at every n . We may now introduce the state-dependent dynamics by allowing the parameters δ, α to be dependent on the step number n and the state of the system at the last step x_n . That is we may take some (pre-defined) functions of two arguments $\alpha(n, x)$, $\delta(n, x)$ and at every step select the parameters for the next step α_{n+1} , δ_{n+1} as: $\alpha_{n+1} = \alpha(n, x_n)$, $\delta_{n+1} = \delta(n, x_n)$. In this way, the parameters p_i , ϵ_i of our random walk are also some pre-defined functions of n , x_n defined by Eqs. (12)-(15).

The functions $\alpha(m, x)$, $\delta(m, x)$ may be quite arbitrary. They add new degrees of freedom to our system, leading, as we will see, to rather interesting new dynamics. We remark also that in quantum control schemes [14] the information about the current state of the system is often used by feeding it back into the system via modification of the system's Hamiltonian. In contrast, in our case, only the parameters of the measurement itself, but not the parameters of system, are changed.

D. Master equation

Using Eqs. (3)-(5) or Eqs. (8)-(9) it is easy to obtain an equation governing the evolution of the probability density function (pdf) $P(n, x)$, describing the probability P of $|q\rangle$ to appear in the vicinity of x at the step n . Since our qubit $|q\rangle$ always remains in a pure state which is fully described by its coordinate x (or, equivalently, by θ), such master equation is just another way to express the dynamics of $|q\rangle$. It provides essentially the same information as Eqs. (3)-(5) or Eqs. (8)-(9). This reformulation will be however useful in the next sections when we consider stochastic ratchet behavior.

We start from the general case with no assumption

about the particular coordinate system. We use the variable y by which we may understand any of the coordinates x , θ or Π mentioned before. We introduce furthermore the measure $d\mathcal{P}(n, y) = P(n, y)dy$ which expresses simply the total probability to find $|q\rangle$ in the interval $[y, y + dy]$. Then, by definition of our process, using the Markov property and the formula for total probability [40] we obtain the following relation:

$$d\mathcal{P}(n+1, y) = p_0(y_0(y))d\mathcal{P}(n, y_0(y)) + p_1(y_1(y))d\mathcal{P}(n, y_1(y)), \quad (16)$$

where $y_i(y)$, $i = 1, 2$ are defined in an implicit way as $y = y_i + \epsilon_i(y_i)$. This expression is valid for an arbitrary (also varying) step size, that is, also for the state-conditioned trajectories as they were defined above in the previous section. In the case of x -coordinates ($y \equiv x$) we obtain straightforwardly the following expression for $P(n, x)$:

$$P(n+1, x) = p_0(x_0(x))x'_0(x)P(n, x_0(x)) + p_1(x_1(x))x'_1(x)P(n, x_1(x)), \quad (17)$$

where $x = x_i(x) + \epsilon_i(x_i(x))$, $x'_i(x) = dx_i(x)/dx$. In particular, for the constant measurement strength we have, $\epsilon_i = \text{const}$, $x'_i(x) = 0$, and therefore we have:

$$P(n+1, x) = p_0(x - \epsilon_0)P(n, x - \epsilon_0) + p_1(x - \epsilon_1)P(n, x - \epsilon_1). \quad (18)$$

Very important are conserved quantities of Eq. (16) or Eq. (17). The most obvious one is the average value of Π on n th step, $\langle \Pi \rangle_n \equiv \int_{-\infty}^{+\infty} \Pi(x)P(n, x)dx$, which represents the a priori probability to find $|q\rangle$ in the state $|1\rangle$ if we perform a projective measurement of $|q\rangle$ after the n -th step of our process. One can show that from Eq. (18) it follows that:

$$\langle \Pi \rangle_{n+1} = \langle \Pi \rangle_n, \quad (19)$$

and thus for any n , $\langle \Pi \rangle_n = \langle \Pi \rangle_0$. Eq. (19) can be obtained by substituting Eq. (17) into definition of $\langle \Pi \rangle_{n+1}$, giving thus

$$\langle \Pi \rangle_{n+1} = \int_{-\infty}^{+\infty} \Pi(x) P(n+1, x) dx = \int_{-\infty}^{+\infty} P(n, x) \{p_0(x)\Pi(x) + p_1(x)\Pi(x)\} dx, \quad (20)$$

where we made a replacement $x'_i(x)dx \rightarrow dx_i$ and the variable change $x_i(x) \rightarrow x$ in both parts of the integral. Since $p_0(x) + p_1(x) = 1$, this gives Eq. (19). We remark that Eq. (19) is universal, that is valid for any choice of the measurement parameters, also if they vary in dependence on the step n or current position x_n .

III. CONTINUOUS DIFFUSIVE LIMIT

A. general equation

The continuous limit arises if we tend the measurement strength to zero. In this case, instead of the discrete equation Eq. (17), a continuous equation arises, with the step numbers n being mapped to a continuous “time” t . If the measurement strength is constant (independent on n) and if this constant strength tends to zero, the corresponding limit is universal, that is, does not depend on the measurement strength and on the particular measurement procedure. The dynamics in such “unconditional” continuous limit is often described by the stochastic Schrödinger equation or by the master equation for the density matrix [14, 17, 18, 22–24, 41]. Nevertheless, to our knowledge, a consideration general enough to include time- and conditionally-varied measurements were presented only very recently in [42]. Earlier works dealt only with the case of measurements of equal strength or at least the strength which is not explicitly time dependent (but might depend on time indirectly via the outcome of the previous measurement) [17, 18]. Instead of directly writing the resulting equation according [42] we will proceed, for the sake of closeness of presentation, from the master equation for $P(n, x)$, derived in the previous section, to the corresponding continuous limit described by the Fokker-Planck (FP) equation. The FP approach used here is also different from [42] where Ito calculus is used, but Ito and FP approaches are, of course, equivalent [40]. We use the later because of the straightforward connection to the methods used in the theory of stochastic ratchets [28].

That is, our goal here is to derive the FP equation in the case which includes the walk with conditionally varying measurement parameters δ , α which depend on the outcome of the all previous measurements and also on n . The transition to the continuous time can be done as follows: We introduce “time” t such that each step of our process corresponds to a small interval $\tau_n = \tau(\delta_n(n, x_{n-1}), \alpha_n(n, x_{n-1}))$, that is, we replace

$$n = \sum_{i=1}^n 1 \text{ by}$$

$$t \equiv \sum_{i=1}^n \tau_i \quad (21)$$

and allow $\tau_i(x_i)$ to tend to zero for every i , x_i . We do not assume that all τ_i are equal. In our case, as $\tau_i(x_i) \rightarrow 0$, we can expect that $P(t, x) \equiv P(n, x)|_{n \rightarrow t}$ changes at every step only slightly and we can then decompose $P(t, x)$ into series as:

$$P(t + \tau_n, x) \cong P(t, x) + \tau_n \partial_t P(t, x). \quad (22)$$

To be allowed to do this we must assume that, independently on n , the step size $\epsilon_{i,n} = \epsilon_i(\delta_n(n, x_{n-1}), \alpha_n(n, x_{n-1}))$ defined in Eqs. (14)-(15) goes to zero as $\tau_n \rightarrow 0$. In particular, this is the case if $\delta_n \rightarrow 0$, $\alpha_n = \text{const}_n > 0$ for all n . Thus, for small enough δ_n , we may assume:

$$\alpha_n = \text{const}(n, x), \quad (23)$$

$$\delta_n = \delta g_\delta(x_{n-1}, n), \quad (24)$$

$$\tau_n = \delta^2 g_\tau(x_{n-1}, n), \quad (25)$$

where we introduced the parameter $\delta \rightarrow 0$ which describes how fast δ_n and τ_n approach to zero; $g_\tau(x, n) > 0$, $g_\delta(x, n)$ are some functions which do not depend on δ and which we can chose at our will.

That is, we require that all τ_n , δ_n tend to zero as $O(\delta^2)$ and $O(\delta)$ respectively. This template is taken from the consideration of the case with the constant step size as shown in Appendix B. The functions $g_\tau(x, n) > 0$ and $g_\delta(x, n)$ provide “form-factors”, which determine the strength of measurement in dependence on the system position x and n . Using Eqs. (21),(24),(25), we define a function $g(x, t)$ as:

$$g(x, t) = \left. \frac{g_\delta(x_{n-1}, n)}{g_\tau(x_{n-1}, n)} \right|_{n \rightarrow t; x_{n-1} \rightarrow x}. \quad (26)$$

Using Eqs. (22),(26) we derive, in a rather standard way, the FP equation (see Appendix C for details and a description of the general procedure in [40]):

$$\partial_t P(t, x) = -\partial_x J(t, x), \quad (27)$$

$$J(x, y) = \mu(t, x)P(t, x) - \partial_x (D(t, x)P(t, x)). \quad (28)$$

Here

$$\mu(x, t) = g(x, t)^2 \tanh(x), \quad D(x, t) = g(x, t)^2 / 2, \quad (29)$$

have now the meaning of the drift and diffusion coefficients, respectively. In different coordinates, like θ or Π the FP equation conserves its form, only the drift and diffusion coefficient modifies (see Sec. D).

This FP equation, as said, describes the dynamics of the pure state $|q\rangle$ which position on the line between $|0\rangle$ and $|1\rangle$ is described by the coordinate x . Stochastic distribution of the position x is due to unpredictable

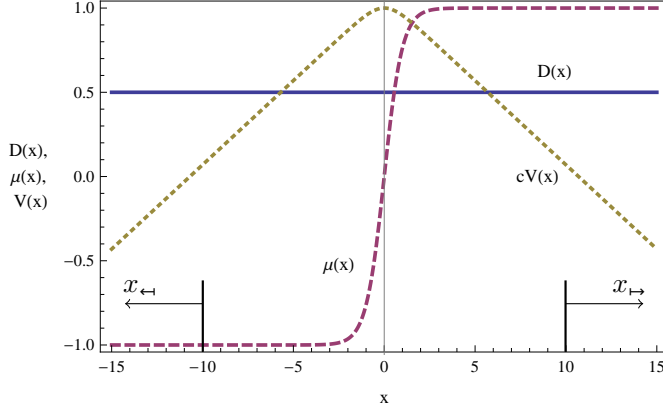


FIG. 2. Diffusion $D(x)$ (solid blue line), drift coefficient $\mu(x)$ (dashed red line) and the effective potential $V(x)$ (dotted yellow line, normalized to a constant $c = 0.1$ for better visibility) in dependence on x according to Eq. (32). The asymptotic coordinates $x_{\leftarrow}, x_{\rightarrow}$ defined in Eqs. (34)-(35) are shown, with $X = -10$ in this case. Asymptotic coordinates are useful when $|x|$ is large, that is, as the step $n \rightarrow \infty$: $D(x)$, $\mu(x)$ and $V(x)$ are significantly simplified for large $|x|$.

character of the weak measurement sequence. The same FP equation describes also a Brownian heavily damped particle moving in the potential

$$V(x, t) = - \int_0^x \mu(x', t) dx', \quad (30)$$

[28, 43]. The average drift velocity $\langle \dot{x}(t) \rangle \equiv \int_{-\infty}^{+\infty} \frac{dx}{dt} P(x, t) dx$ can be obtained also as an average of $J(x, t)$:

$$\langle \dot{x}(t) \rangle = \int_{-\infty}^{+\infty} J(x, t) dx. \quad (31)$$

Note that here the ensemble average is assumed, and $\langle \dot{x}(t) \rangle$ depends on t . For the case of $g(x) = 1$, that is, if the step size in our random walk is state-independent, we have:

$$\mu(x) = \tanh(x), \quad V(x) = \ln(\cosh(x)), \quad D = \frac{1}{2}. \quad (32)$$

The corresponding functions μ , D , V are shown in Fig. 2. The solution of Eqs. (27)-(28), (32) with the initial condition $P(0, x) = \delta(x - X)$, where $\delta(x - X)$ is the Dirac delta-function localized at the arbitrary point X can be found analytically [23]:

$$P(t, x) = \frac{1}{\sqrt{2\pi t}} \frac{\cosh x}{\cosh X} \exp\left(-\frac{t^2 + (x - X)^2}{2t}\right). \quad (33)$$

B. Asymptotic FP equation

To make a semi-analytic approach described in [28] working (as described in the next section), we have to

find the conditions where, assuming $g = \text{const}$ in Eq. (32), we have also $\mu = \text{const}$. In our equations this is generally not the case because of $\tanh(x)$ factor. However, as one can see from Fig. 2 and from Eq. (32), the deviation from this condition decreases exponentially with $|x|$ because $|\tanh(x)|$ exponentially fast approaches 1. Also, as one can see from Eq. (33), if we take the initial starting point X far away from the origin $X = 0$, $P(t, x)$ behaves very much like a normal Gaussian distribution which shifts with time with the constant unit speed away from $x = X$, and expands with the variance $\sigma^2 = t$.

This allows us to consider the asymptotic behavior, as the initial point X and thus x are far enough from the origin $x = 0$. We thus introduce “shifted” coordinates $x_{\leftarrow}, x_{\rightarrow}$ as (see also Fig. 2):

$$x_{\leftarrow} = x + X, \quad (34)$$

$$x_{\rightarrow} = x - X, \quad (35)$$

where $X \gg 0$ is a large arbitrary number. We will call them “asymptotic coordinates”. For such defined variables, neglecting the terms which is exponentially small with $|X|$ we have from Eq. (29):

$$\mu(x_{\leftarrow}, t) = -g(x_{\leftarrow}, t)^2, \quad \mu(x_{\rightarrow}, t) = g(x_{\rightarrow}, t)^2, \quad (36)$$

$$D(x_{\leftarrow}, t) = g(x_{\leftarrow}, t)^2/2, \quad D(x_{\rightarrow}, t) = g(x_{\rightarrow}, t)^2/2, \quad (37)$$

that is, the factor $\tanh(x)$ which were present in the diffusion coefficient in Eq. (32), disappears. In the following, we will consider only the case when $x \rightarrow -\infty$, and, correspondingly, we restrict ourselves to the variable x_{\leftarrow} (cf. Fig. 2). The dynamics for the case of $x \rightarrow +\infty$ is obviously analogous, only the overall drift direction will be the opposite as Eq. (36) indicates. The asymptotic FP equation for this case coincides with the original one Eqs. (27)-(28), only written in asymptotic coordinates $x \rightarrow x_{\leftarrow}$:

$$\partial_t P(t, x_{\leftarrow}) = -\partial_{x_{\leftarrow}} J(t, x_{\leftarrow}), \quad (38)$$

$$J(x_{\leftarrow}, y) = \mu(t, x_{\leftarrow}) P(t, x_{\leftarrow}) - \partial_{x_{\leftarrow}} (D(t, x_{\leftarrow}) P(t, x_{\leftarrow})). \quad (39)$$

C. FP equation for periodically varying potential

In this section we focus on the case when $g(x_{\leftarrow}, t)$ changes in space and time periodically. We assume g to have period L in space x_{\leftarrow} . In our new asymptotic coordinates, reformulation of the FP equation Eqs. (36)-(39) allowing to take advantage of such periodicity is possible [28]. Namely, we define the reduced quantities:

$$\tilde{P}(x_{\leftarrow}, t) = \sum_{j=-\infty}^{+\infty} P(x_{\leftarrow} + jL, t), \quad (40)$$

$$\tilde{J}(x_{\leftarrow}, t) = \sum_{j=-\infty}^{+\infty} J(x_{\leftarrow} + jL, t). \quad (41)$$

Obviously, $\tilde{P}(x_{\leftarrow}, t)$ and $\tilde{J}(x_{\leftarrow}, t)$ are finite and defined in the range $x_{\leftarrow} \in [-L/2, L/2]$. Moreover, from Eqs. (40)-(41) one can see that \tilde{P}, \tilde{J} are periodic in x_{\leftarrow} :

$$\tilde{P}(x_{\leftarrow}, t) = \tilde{P}(x_{\leftarrow} + L, t), \quad \tilde{J}(x_{\leftarrow}, t) = \tilde{J}(x_{\leftarrow} + L, t). \quad (42)$$

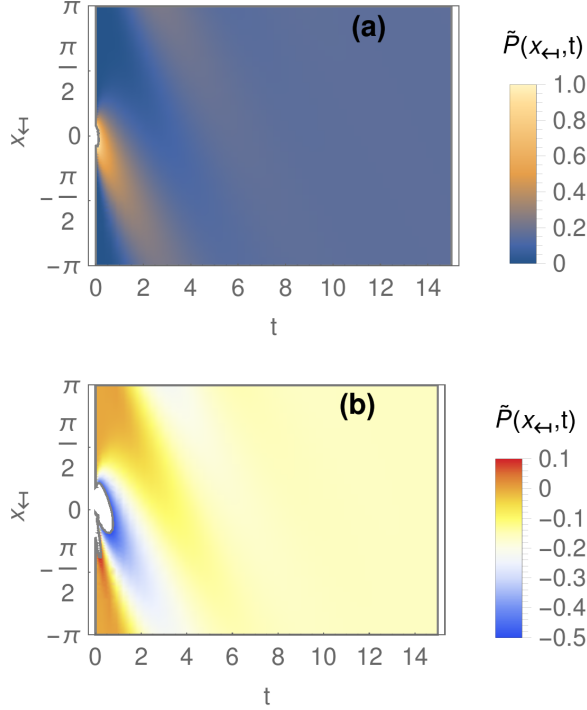


FIG. 3. The dynamics of the reduced asymptotic probability density $\tilde{P}(t, x_{\leftarrow})$ (a) and the current density $\tilde{J}(t, x_{\leftarrow})$ (b) for $g(t, x_{\leftarrow}) = 1$ obtained by direct simulations of Eqs. (43)-(44), assuming periodic boundary conditions and initial conditions described in text. In contrast to initial variables P, J , the reduced variable \tilde{P}, \tilde{J} do have a steady-state, which is in this case a homogeneous distribution.

In the asymptotic variables $\{x_{\leftarrow}, t\}$, as it follows from Eqs. (36)-(37), $\mu(x_{\leftarrow}, t)$ and $D(x_{\leftarrow}, t)$ are periodic in space with the same period L (which is by the way not true for μ and D written using the original variable x). Under these circumstances the FP equation written for \tilde{P}, \tilde{J} remains the same as for P, J . That is, we have:

$$\partial_t \tilde{P}(t, x_{\leftarrow}) = -\partial_{x_{\leftarrow}} \tilde{J}(t, x_{\leftarrow}), \quad (43)$$

$$\tilde{J}(x_{\leftarrow}, t) = \mu(t, x_{\leftarrow}) \tilde{P}(t, x_{\leftarrow}) - \partial_{x_{\leftarrow}} (D(t, x_{\leftarrow}) \tilde{P}(t, x_{\leftarrow})), \quad (44)$$

where the coefficients remain the same as before, that is, are given by Eqs. (36)-(37). The advantage of such reformulation is that now we can consider only the finite interval in x_{\leftarrow} from, say, $-L/2$ to $L/2$. Besides, the equation for the average drift velocity Eq. (31) also retains its form:

$$\langle \dot{x}_{\leftarrow}(t) \rangle = \int_{-L/2}^{L/2} \tilde{J}(x_{\leftarrow}, t) dx. \quad (45)$$

Remarkably, the direct definition of $\langle \dot{x}_{\leftarrow}(t) \rangle$ as the average of \dot{x}_{\leftarrow} with the probability distribution $\tilde{P}(x_{\leftarrow}, t)$ is not valid anymore.

As an illustration of the dynamics appearing in the reduced equations, we show in Fig. 3 the dynamics of $\tilde{P}(x_{\leftarrow}, t), \tilde{J}(x_{\leftarrow}, t)$ for the case of $g(x_{\leftarrow}, t) = \text{const} = 1$ obtained using direct numerical simulations of Eqs. (43)-(44) with the initial condition $P(x_{\leftarrow}, t) \propto \exp(-x_{\leftarrow}^2/0.1)$ and periodic boundary conditions. The figure shows rather rapid homogenization of $\tilde{P}(x_{\leftarrow}, t), \tilde{J}(x_{\leftarrow}, t)$ in space because of the action of diffusion. This homogenization illustrates an important peculiarity of the reduced quantities: although the initial variables J, P have no steady-state in their dynamics, the reduced quantities \tilde{J}, \tilde{P} do have a steady-state. In the case of Fig. 3 this steady state is simply a constant which does not depend neither on t nor on x_{\leftarrow} .

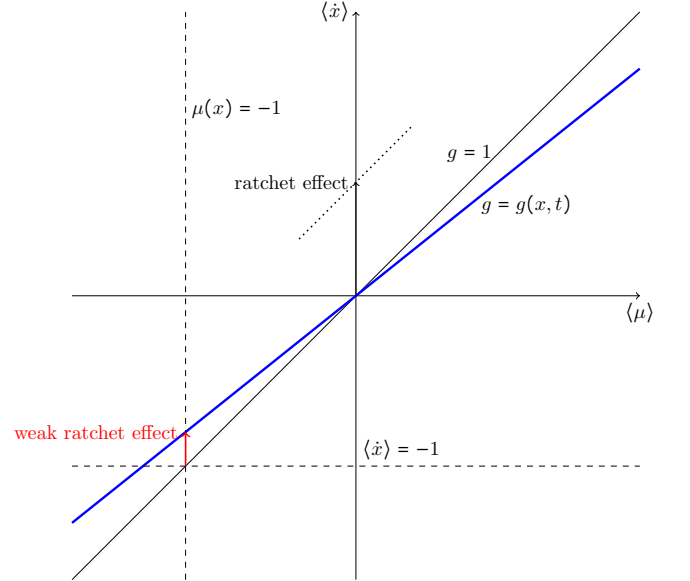


FIG. 4. Schematic representation of the Brownian ratchet effect. Without a ratchet effect ($g = 1$), a constant drift force μ leads to a current $\langle \dot{x} \rangle = \mu$ (black thin line). In contrast, when g changes in space and/or time (but still $\langle g \rangle = 1$), the average current $\langle \dot{x} \rangle$ can be modified even through the average force $\langle \mu \rangle$ remains the same (blue solid and black dotted lines). Although in many other systems the Brownian ratchet effect can change the average direction of motion (see black dotted line), it is not possible in the present case – the type of ratchet which we call “weak ratchet”. In this later case, $|\langle \dot{x} \rangle|$ can be modified but its sign is not reversed (see blue line). The asymptotic values of μ and $\langle \dot{x} \rangle$ for $x \rightarrow -\infty$ (that is, assuming asymptotic coordinates x_{\leftarrow}) are marked by dashed lines. Weak ratchet effect in the asymptotic case is marked by a red arrow.

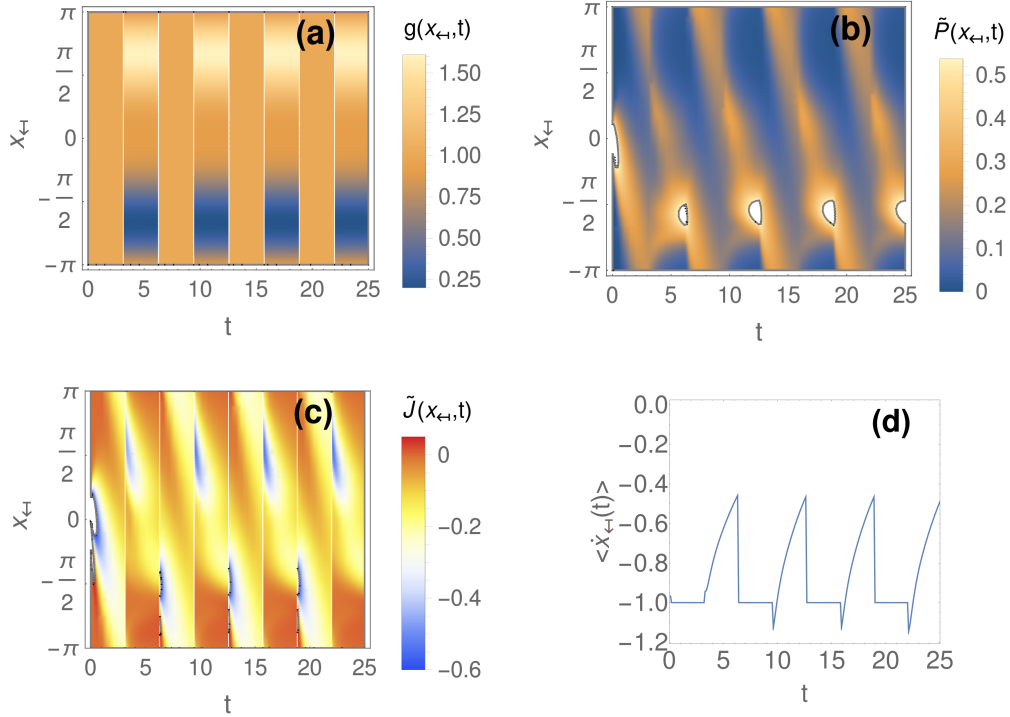


FIG. 5. Brownian ratchet effect for $g(x_{\leftarrow}, t)$ varying in space and time. (a) $g(x_{\leftarrow}, t)$, as given by Eqs. (50)-(53). (b), (c) the reduced asymptotic probability density $\tilde{P}(x_{\leftarrow})$ and the current density $\tilde{J}(x_{\leftarrow})$ obtained by direct simulations of Eqs. (43)-(44) with periodic boundary conditions and initial conditions described in text. (d) the averaged current $\langle \dot{x}_{\leftarrow}(t) \rangle$ in dependence on time.

IV. BROWNIAN RATCHETS

One of the most interesting phenomena in Brownian flows is a possibility of so called stochastic ratchets [27, 28]. Namely, by manipulating dynamically the potential $V(x, t)$ in a Brownian flow, one can have nonzero average motion $\langle \dot{x} \rangle \neq 0$ even in the case when the average force, $\langle \mu \rangle \equiv \int \mu(x, t) dx$ is exactly zero (for every t). Here, to simplify notations, we used the denotation $\langle \dot{x} \rangle$ for the time- and space average defined as:

$$\langle \dot{x} \rangle \equiv \langle \bar{\dot{x}}(\infty) \rangle, \quad (46)$$

where:

$$\langle \bar{\dot{x}}(t) \rangle \equiv \frac{1}{t} \int_0^t \langle \dot{x}(\tau) \rangle d\tau \quad (47)$$

is the "moving average" in time of the space average. Alternatively, one can speak about a ratchet effect if a nonzero initial force $\mu \neq 0$ can be canceled or even reversed by introducing some periodic modulations of the potential. Both of these definitions are visualized in Fig. 4.

In our case it is quite clear that the average flow defined by $\mu = -1$ (in the asymptotic case $x \rightarrow x_{\leftarrow}$) can not be reversed. Otherwise, one would have a possibility to violate the conservation law of $\langle \Pi \rangle$ given by Eq. (19) by

tuning, for every particular trajectory, the potential in such a way that the current system state is forced to move in the direction opposite to μ and thus bring our system to any of the states $|0\rangle$, $|1\rangle$ at our wish which would violate Eq. (19).

Nevertheless, one can try to find a Brownian ratchet effect in a weak sense, that is, to find such a function $g(x_{\leftarrow}, t)$ that the asymptotic value of $\langle \dot{x}_{\leftarrow} \rangle > -1$, despite of $\langle \mu \rangle = -1$. The notion of a weak ratchet effect, in comparison to a "normal" stochastic ratchet, is visualized in Fig. 4 (blue line). Weak ratchets are in close correspondence to the weak Parrondo games, where the combination of lossy games lead to less lossy one, but still not to a winning one [30]. Of course, one can always obtain $\mu(x_{\leftarrow}, t) = 0$ by simply putting $g = 0$, that is, by reducing step size of the random walk to zero. Here we want however to investigate the effects which is independent on such raw step size reduction. To ensure this we will always take such g that

$$\langle g(t)^2 \rangle = 1, \quad (48)$$

where we define $\langle g(x_{\leftarrow}, t)^2 \rangle$ as:

$$\langle g(t)^2 \rangle \equiv \frac{1}{L} \int_{-L/2}^{L/2} g(x_{\leftarrow}, t)^2 dx_{\leftarrow}. \quad (49)$$

This condition excludes the possibility to reduce $\langle \dot{x}_{\leftarrow} \rangle$ by

reducing the measurement strength globally. That is, if one reduces the measurement strength near some point, one has to increase it in the vicinity of some another one.

We will now try to construct a periodic in time and space function g which allows to reduce $\langle \dot{x}_\leftarrow \rangle$, making it as small as possible.

We remark that several various types of stochastic ratchets has been considered in the literature (see [28, 29] and references therein), the classification is based on the functional form of D and μ . In many commonly studied hydrodynamic Brownian flows μ and D can be varied quite independently – in contrast to our situation where independent variation of D and μ is impossible because of the common factor g . Our situation closely resembles hydrodynamic Brownian ratchets with varying friction [28, 44–46]. The most studied class of ratchets is so called pulsating ones, where μ may vary in space and time, whereas D is a constant. On the other hand, the situations when both μ and D vary in space or, alternatively, in time, were also considered under the names Seebeck or temperature ratchets, correspondingly. They can be mapped, by suitable change of variable, to the pulsating ratchets.

In our case, as one can see, the situation when g is changing in time but not in space provides no possibility for any ratchet effect. Namely, in this case Eq. (45) can be calculated directly by integrating Eq. (44) with the boundary conditions Eq. (42), giving $\langle \dot{x}_\leftarrow(t) \rangle = -1$. We have then $\tilde{P} \rightarrow \text{const} = 1/L$, that is, full homogenization of \tilde{P} will take place, exactly as in the case of $g = 1$.

We can therefore consider the cases when μ and D change both in time and space or only in space. For the presence of the ratchet effect, the symmetry of the μ and D are of the critical importance. In general, “almost all” functions except the ones processing certain particular symmetry properties allow the ratchet effect [28, 29]. Nevertheless, no analytical symmetry relation is known, to our knowledge, for the case when both μ and D are arbitrary functions of space and time. For the case when μ and D are only space-dependent, the situation is simpler and is discussed in the next section.

One of the most well-known types of ratchets is an on-off tilting ratchet, where the diffusion D is constant and the asymmetric potential V is switched on and off. At the on-stage, the particle moves to the minimum of the potential and therefore becomes well localized. When the potential is switched off, diffusion leads to a broadening of the particle’s wave packet. Switching the potential on again makes the particle feeling the force, which pushes it to certain direction. If the potential is asymmetric, the force is also asymmetric, leading to an average current.

Having in mind said above, we first probe functions $g(x_\leftarrow, t)$ which has the following form:

$$g(x_\leftarrow, t) = C(t) \{1 + F(x_\leftarrow) f(t)\}, \quad (50)$$

where the function $f(t)$ is periodic in time which models the switching on and off behavior, and $F(x)$ is periodic in space, but might be asymmetric. The normalizing

constant $C(t)$ is obtained from Eq. (48). To start with, we will try the following functions:

$$f(t) = (\text{sign}(\sin(t)) - 1)/2, \quad (51)$$

$$F(x_\leftarrow) = a [\sin(x_\leftarrow) + b \sin(2x_\leftarrow)], \quad (52)$$

$$a = -0.6, b = -0.5. \quad (53)$$

Here, $f(t)$ works as a switcher which is active only half of the period, a determines the “amplitude” of the periodic potential whereas b is selected in such a way that the shape of g resembles a “saw-tooth” one, in order to introduce some spatial asymmetry into the profile g . Indeed, this shape of F is simply the decomposition of the ideal saw-tooth shape $F_s(x) = \sum_{n=1}^{\infty} (-1)^n \sin nx/n$ which is cut off on the second term.

The resulting dynamics is plotted in Fig. 5. Namely, the shape of g is presented in Fig. 5(a) whereas Fig. 5(b) and Fig. 5(c) show the temporally- and spatially resolved probability and current. To calculate Fig. 5, the boundary and initial conditions were taken as in Fig. 3. One can see from Fig. 5(b) that when the space-varying potential is on, the probability density \tilde{P} concentrates in the regions where g (and thus D, μ) is minimal. When it is off, the wave packet starts to diverge (and at the same time is moving to the negative direction of x_\leftarrow). This behavior is thus different from typical pulsating ratchets in the sense that when the potential is switched on, the particle is localized in the minima of g (and thus of D and μ and not in the minima of the potential. In Fig. 5(d) one can see that the current $\langle \dot{x}_\leftarrow(t) \rangle$ approaches, after a short transition process, a stationary regime of oscillations in time with a period 2π . The long time behavior of the average of $\langle \dot{x}_\leftarrow(t) \rangle$ given by Eq. (47) is shown in Fig. 6, where it is seen that this average approaches ≈ -0.86 instead of -1 as in the case of constant $g = 1, \mu = -1$, thus clearly showing the ratchet effect in this process.

To check the stability of the effect, simulations were made for different functions $f(t), F(x)$. For instance, in Fig. 6 the case with $b = 0$ and $f(t) = \text{sign}(\sin(t))$ is also plotted. In this case, the ratchet effect is definitely smaller but still persists. As said, the condition Eq. (48) excludes the effect of bare step size reduction in this random walk, demonstrating that the ratchet effect is a dynamical phenomenon independent from the step size.

V. SEEBECK RATCHETS AND DYNAMICAL LOCALIZATION

In general, the ratchet effect can appear if D, μ change only in space. In this case, one may have the diffusion D and the potential V defined by Eq. (30) being not in phase [28], which is in our case is typically fulfilled, since $D \sim \mu, \mu = -\partial_x V$ (that is, if $D \sim \sin x$, then $V \sim \cos x$; see also Fig. 8). Such ratchets are typically known as Seebeck ones [28]. For Seebeck ratchets, an analytical condition exists which determines the absence of the ratchet effect. In particular, if we consider the case with no average

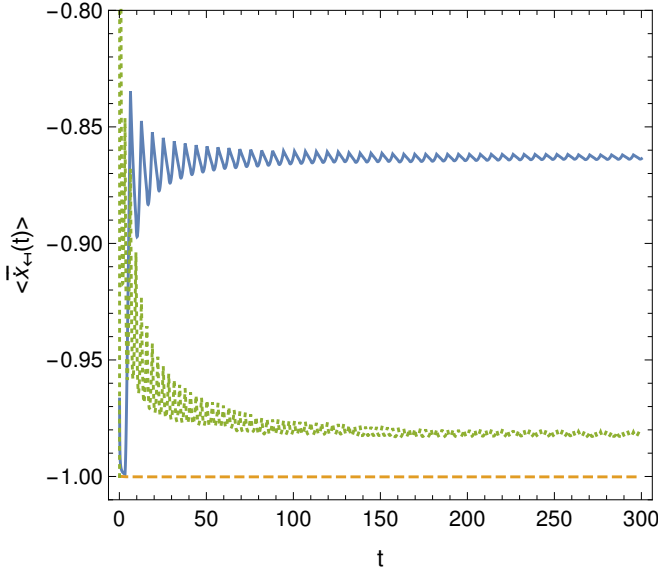


FIG. 6. Dependence of the temporal average $\langle \bar{x}_{\leftarrow} \rangle$ given by Eq. (47) on the averaging time interval t . In the case of constant $g = 1$ (orange dashed line) this quantity quickly approaches -1 (no ratchet effect), whereas in the case of varying measurement strength with the parameters Eqs. (50)-(53) (blue solid line) it approaches ≈ -0.86 , demonstrating a weak Brownian ratchet. The effect strength depends on the function shape. For instance, green dotted line shows the case Eq. (50) with the spatial dependence $F(x)$ given by Eq. (52) with $a = -0.8$, $b = 0$, and $f(t) = \text{sign} \sin t$.

force ($\langle \mu \rangle = 0$) and if $\int_{-L/2}^{L/2} \mu(x)/D(x)dx = 0$, no ratchet effect is present [47, 48]. In our case, $\langle \mu \rangle \neq 0$ so that the condition above can not be applied directly. Nevertheless, we can, by the replacement $x_{\leftarrow} \rightarrow x_{\leftarrow}, t \rightarrow t - x_{\leftarrow}$, reduce our equation to the case with $\langle \mu \rangle = 0$. In this case we have $\langle \dot{x}_{\leftarrow} \rangle \rightarrow \langle \dot{x}_{\leftarrow} \rangle + 1$. Afterwards, we can apply the above criterion, which gives us the criterion for the absence of the ratchet effect for our case in the form:

$$\frac{1}{L} \int_{-L/2}^{L/2} \frac{1}{g^2(x_{\leftarrow})} dx_{\leftarrow} = 1. \quad (54)$$

That is, for a typical function g (which satisfies Eq. (48)) we should expect the presence of a ratchet effect, unless Eq. (54) is also valid. An exemplary profile of g which we use to test the Seebeck ratchet numerically is given by Eq. (50) with $f(t) = 1$ and $F(x_{\leftarrow})$ defined by Eq. (52) with:

$$a = -0.8, b = 0, \quad (55)$$

and is shown in Fig. 7(a). For such a function g , as one can see in Fig. 7(b), the average current $\langle \dot{x}_{\leftarrow} \rangle$ can be also larger than -1 ; in the case of Fig. 7 it approaches ≈ -0.2 as one can see in Fig. 7(d). In this case, the initial distribution is quickly rearranged to a stationary (but inhomogeneous) one.

Now, again, the system is located mostly near the minimum of g . This allows interpretation of the Seebeck

ratchet effect in the present case in the terms of a "dynamical localization". Namely, let us observe the potential $V(x_{\leftarrow})$ as shown in Fig. 8 (solid blue line). One can see that $V(x_{\leftarrow})$ approaches a flat region (where it is almost constant) close to $x_{\leftarrow} = \pi/2$. That is, there is almost no effective force at that point. If our effective "particle" approaches this region, it nearly stops. Nevertheless, the "particle" experiences some small drift to the negative direction of x_{\leftarrow} .

Going one step further, we consider now the case when $g = 0$ at some point. In this case we also expect localization shown in the previous example. But more interesting dynamics will also appear as we will see below. In general, to observe localization, it is not necessary to take the periodic potential as it was in the previous example. We now consider the global dynamics related to localization, and therefore we return back from "asymptotic coordinate" x_{\leftarrow} to the initial coordinate x and thus to the FP equation as written in Eqs. (27)-(28). We assume also for simplicity that $g(x)$ approaches zero only in one single point X , that is, $g \rightarrow 0$ as $x \rightarrow X$. Returning to our initial qubit, the state $|X\rangle$ is given by

$$|X\rangle = A|0\rangle + B|1\rangle; \quad (56)$$

$$A = \sqrt{\Pi(X)}, B = \sqrt{1 - \Pi(X)}, \quad (57)$$

where $\Pi(X)$ is given by Eq. (11). As we will see later the trajectory can not cross $|X\rangle$ in this case. A state $|x\rangle$ located between of $|0\rangle$ and $|X\rangle$ will approach either $|0\rangle$ or $|X\rangle$ as $t \rightarrow \infty$. Analogously, a state located initially between $|X\rangle$ and $|1\rangle$ will approach either $|X\rangle$ or $|1\rangle$ (see Fig. 9(b)). We note a similarity to the initial system with the state-independent coupling strength $g = 1$ in this limiting dynamics (where the limiting states are $|0\rangle$ and $|1\rangle$, see Fig. 9a). One can make this analogy exact by considering the FP equation in coordinates $\Pi(x)$ defined in Eq. (11) which is given by (see also Sec. D):

$$\partial_t P(t, \Pi) = \partial_{\Pi\Pi} (D(\Pi)P(t, \Pi)) \quad (58)$$

$$D(\Pi) = 2(\Pi - 1)^2 \Pi^2 g^2(\Pi), \quad (59)$$

so that the diffusion coefficient $\mu = 0$ in these coordinates. We remark that for $|0\rangle$ and $|1\rangle$ ($\Pi = 0$ and $\Pi = 1$ correspondingly) $D(\Pi) = 0$.

Let us make the denotation $\Pi(X) \equiv \Pi_X$; we have thus $g(\Pi_X) = 0$. We also consider only one case when the initial state is in between $|0\rangle$ and $|X\rangle$, that is, $x(t = 0) < X$ and $\Pi(t = 0) < \Pi_X$ (see Fig. 9(b), red lines). In this case we can obviously define such function $\tilde{g}(\Pi)$ that:

$$g(\Pi) = \frac{\Pi_X - \Pi}{1 - \Pi} \tilde{g}(\Pi), \quad (60)$$

which is possible without singularities since $1 - \Pi > 1 - \Pi_X > 0$. Here, $\tilde{g} \geq 0$ does not anymore necessarily approaches to zero as $\Pi \rightarrow \Pi_X$. Now, by making a variable change:

$$\tilde{\Pi} = \Pi/\Pi_X, \tilde{t} = \Pi_X^2 t, \quad (61)$$

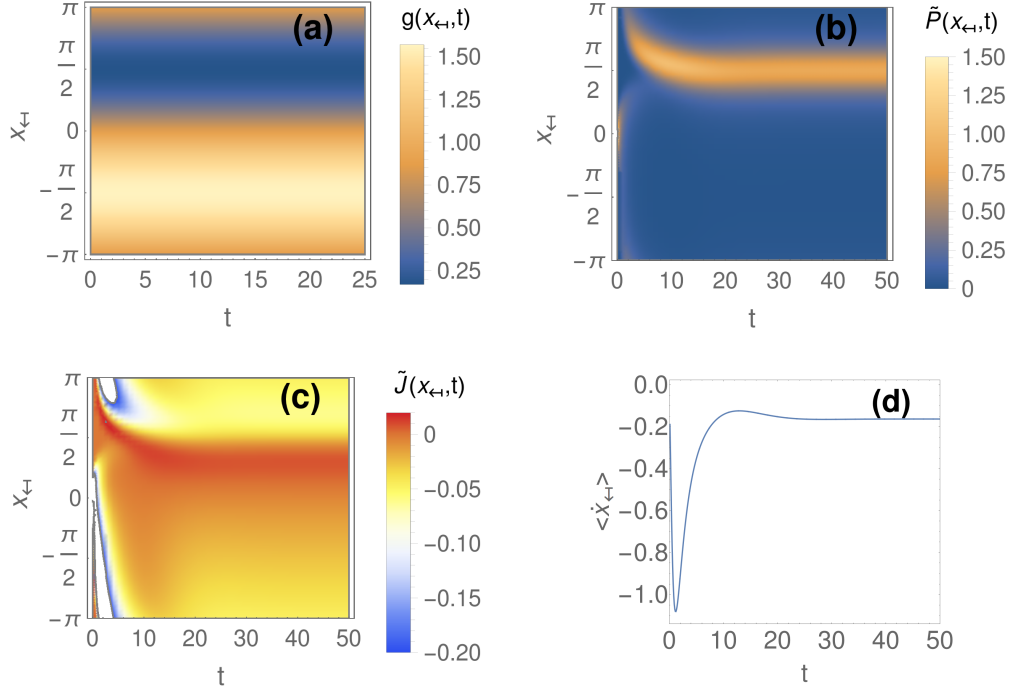


FIG. 7. Seebeck ratchet and dynamical localization effect for $g(x_-)$ dependent only on spatial coordinate. (a) $g(x_-, t)$ given by Eq. (50) with $C(t) = \text{const}$, $f(t) = 1$, and other parameters defined by Eq. (52), Eq. (55). (b), (c) Reduced asymptotic probability density $\tilde{P}(x_-)$ and the current density $\tilde{J}(x_-)$ obtained by direct simulations of Eqs. (43)-(44) with periodic boundary conditions and initial conditions described in text. (d) Spatially averaged current $\langle \dot{x}_- \rangle$ in dependence on time.

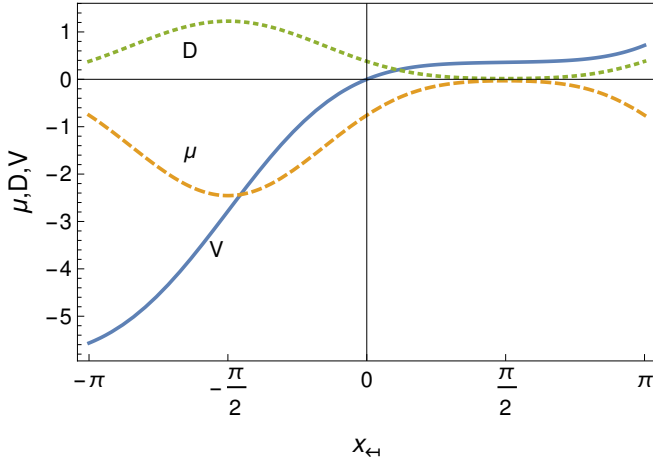


FIG. 8. Diffusion $D(x)$ (solid blue line), shift $\mu(x)$ (dashed red line) and the effective potential $V(x)$ (dotted yellow line, normalized to a constant $c = 0.1$ for better visibility) in dependence on x_- with $g(x_-)$ being time-independent, that is, given by Eq. (50) with $C(t) = \text{const}$, $f(t) = 1$, and other parameters defined by Eq. (52), Eq. (55).

we arrive to a new FP equation:

$$\partial_{\tilde{t}} P(\tilde{t}, \tilde{\Pi}) = \partial_{\tilde{\Pi}\tilde{\Pi}} (\tilde{D}(\tilde{\Pi}) P(\tilde{t}, \tilde{\Pi})), \quad (62)$$

$$\tilde{D}(\tilde{\Pi}) = 2(\tilde{\Pi} - 1)^2 \tilde{\Pi}^2 \tilde{g}^2(\tilde{\Pi}), \quad (63)$$

where $\tilde{g}(\tilde{\Pi}) = \tilde{g}(\Pi/\Pi_X)$. One can see that Eqs. (58)-(59) and Eqs. (62)-(63) are completely equivalent. That is, the dynamics of the random walk between $|0\rangle$ and $|X\rangle$ and between $|0\rangle$ and $|1\rangle$ can be one-to-one-mapped to each other. In particular, the dynamics of the random walk with $\tilde{g} = 1$, that is, with $g(\Pi) = (\Pi_X - \Pi)/(1 - \Pi)$, is completely equivalent to the dynamics of the simplest random walk with $g = 1$. The system with $\tilde{g} = 1$ behaves near $|X\rangle$ in the same way as the system with $g = 1$ near the state $|1\rangle$, for instance, the time of arrival to the point $|X\rangle$ is infinite. This is obviously true for any other bounded functions \tilde{g} obeying Eq. (48) and such that $g > 0$.

This allows also to calculate straightforwardly the probability of the outcomes $|0\rangle$ or $|X\rangle$ (resp. $|X\rangle$ or $|1\rangle$) as $t \rightarrow \infty$. In our initial system with $g = 1$ the a priori probabilities to have $|0\rangle$ or $|1\rangle$ would be given by $\Pi(x)$ and $1 - \Pi(x)$, correspondingly, and, according to Eq. (19), also do not depend on the measurement strength $g(x, t)$ (unless g approaches zero somewhere). By rescaling the latter situation using Eq. (61) we see, that, starting from the state $|x\rangle$ we reach $|0\rangle$ or $|X\rangle$ (resp. $|X\rangle$ and $|1\rangle$) with the probabilities $\tilde{\Pi}(x) = \Pi(x)/\Pi_X$ and $1 - \tilde{\Pi}(x) =$

$1 - \Pi(x)/\Pi_X$. This probability also does not depend on the measurement strength (unless it approaches zero somewhere else at $x < X$). In the same way, if $|x\rangle$ is in between $|X\rangle$ and $|1\rangle$, we obtain that the probabilities to reach $|X\rangle$ or $|1\rangle$ are $(\Pi(x) - \Pi_X)/(1 - \Pi_X)$ and $(1 - \Pi(x))/(1 - \Pi_X)$ respectively.

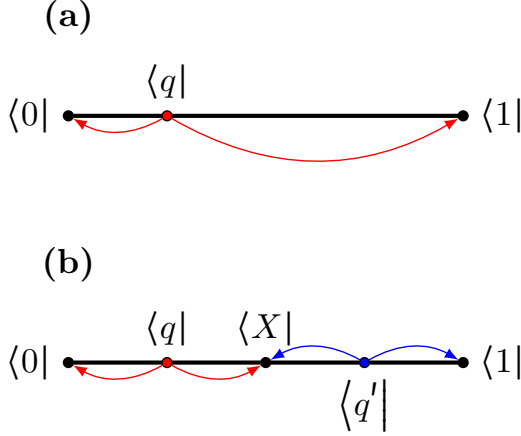


FIG. 9. The limits $t \rightarrow \infty$ of the weak measurement sequence in the case of $g = 1$ (a) and in the case of $g(x, t)$ such that $g(x) \rightarrow 0$ as $x \rightarrow X$ (b); the coordinate X corresponds to the qubit state $|X\rangle$. In the former case, an arbitrary state $|q\rangle$ approaches either to $|0\rangle$ or $|1\rangle$, whereas in the case (b) the state may also have $|X\rangle$ as a limiting point. Some states (such as $|q\rangle$) tend to either $|0\rangle$ or $|X\rangle$, the others (as $|q'\rangle$) approach $|1\rangle$ or $|X\rangle$.

VI. CONCLUSIONS

In the present article we have considered quantum trajectories resulting from a sequence of weak measurements, in the simplest one-dimensional settings, but assuming the measurement strength depending on the step number n and on the current state of the system described by the coordinate x on the line. Of course, the current state can not be inferred from the measurement directly, in contrast to classical systems. Nevertheless, if the initial state and the parameters of the weak measurements are known, all the subsequent positions of the system can be inferred from the sequence of the measurement outcomes, and thus the conditional measurement strength can be well defined.

Such measurement process, in the limit of infinitely small steps, leads to a diffusive dynamics with the both drift and diffusion depending on the coordinate x and time t . In fact, the dynamics arising in such case is quite similar to, for instance, overdamped Brownian particle in a flow with the varying friction coefficient. In this article we discussed the nontrivial dynamics arising due to this analogy.

For instance, an exciting phenomenon arising in Brow-

nian flows is the stochastic ratchet effect, which allows to “rectify” Brownian motion using periodically varying potential. Such potential does not introduce any net force by itself, nevertheless allowing to push particles in the direction opposite to the flow. As it has been shown here, in our case we can achieve only a weak form of the stochastic ratchet effect. That is, we can not reverse the overall drift direction of the quantum trajectories, but only slow down this motion. The ratchet effect manifests itself in the localization of the “particle” in the areas where the measurement strength is reduced and thus the effective force is minimal.

Finally, we considered the case when the step size approaches zero as the system approaches some state $|X\rangle$. No quantum trajectory can cross the singularity point arising in this case. Moreover, the trajectories approach such singularity in the infinite time in a similar way as they approach the “normal” basis states. The FP equation demonstrate remarkable self-similarity in this case: The arbitrary quantum walk between any subsequent zeros can be mapped to a quantum walk between $|0\rangle$ and $|1\rangle$ with the non-vanishing measurement strength.

The effects predicted here can be tested in the measurement-only quantum control settings, such as, for instance, the one recently realized experimentally using defect-in-diamond-based qubits [2], but also in other setups where weak quantum measurement or control was realized, for instance for photon-based [25], ultracold-atom-based [1, 9] or superconducting-based qubits [3].

ACKNOWLEDGMENT

The author is thankful to Nieders. Vorab, project ZN3061, and to German Research Foundation (DFG), project BA 4156/4-1, for the financial support.

Appendix A: Derivation of the expression for step size

To derive the step size $\epsilon_i(x_n) \equiv x_{n+1} - x_n$ on the n th step of our random walk, we use Eqs. (3)-(7) and the relation:

$$\sin^2 \theta_n = \frac{1 + \tanh x_n}{2}. \quad (\text{A1})$$

For instance, in the case if the measurement of the ancilla $|a\rangle$ is $|0\rangle$, we have from Eqs. (3)-(7):

$$\sin \theta_{n+1} = \sin \theta_n \cos(\delta + \alpha)/\sqrt{p_0}, \quad (\text{A2})$$

and thus, using Eq. (A1):

$$\frac{1 + \tanh x_{n+1}}{2} = \frac{(1 + \tanh x_n) \cos^2(\delta + \alpha)}{2p_0}. \quad (\text{A3})$$

Hence, the expression for $\epsilon_0(x)$ (redefining x_n as x since x_n is arbitrary) is:

$$\epsilon_0(x) = \operatorname{atanh} \left(\frac{(1 + \tanh x) \cos^2(\delta + \alpha)}{p_0(x)} - 1 \right) - x. \quad (\text{A4})$$

In the same way, if $|a\rangle$ collapses to $|1\rangle$ upon the measurement, we have

$$\sin \theta_{n+1} = \sin \theta_n \sin(\delta + \alpha) / \sqrt{p_1}, \quad (\text{A5})$$

and thus we obtain for $\epsilon_1(x)$:

$$\epsilon_1(x) = \operatorname{atanh} \left(\frac{(1 + \tanh x) \sin^2(\delta + \alpha)}{p_1(x)} - 1 \right) - x. \quad (\text{A6})$$

Now we calculate analytically the expression for $d\epsilon_i(x)/dx$, which can be straightforwardly shown to be zero. Thus, $\epsilon_i(x) = \epsilon_i(0) \equiv \epsilon_i$ and we can take $x = 0$ in Eq. (A4), Eq. (A6), thus obtaining expressions Eqs. (14)-(15).

Appendix B: Quantum trajectories with constant measurement parameters

In the case of a constant x -independent step (and only in this case) it is constructive to analyze ϵ_i , p_i on more general level by introducing the “average step” $\mu(x)$:

$$\mu(x) = \mu_0(x) + \mu_1(x), \quad \mu_i(x) = \epsilon_i p_i(x), \quad i = 0, 1. \quad (\text{B1})$$

μ defines an “average direction” of evolution: towards $+\infty$ or $-\infty$.

Equations Eq. (B1) are simplified when δ is small (assuming fixed $\alpha > 0$), so we can decompose Eqs. (12)-(15) in series in δ . In this case, up to the second order of δ we have:

$$\mu(x) = \delta^2 \tanh(x) + O(\delta^3), \quad (\text{B2})$$

$$2\mu_0(x) = \delta \sin(2\alpha) + \delta^2 (4\Pi(x) \sin^2 \alpha - 1) + O(\delta^3), \quad (\text{B3})$$

$$2\mu_1(x) = -\delta \sin(2\alpha) + \delta^2 (4\Pi(x) \cos^2 \alpha - 1) + O(\delta^3), \quad (\text{B4})$$

where $\Pi(x)$ is given by Eq. (11). Since $\operatorname{sign} x = \operatorname{sign} \tanh x$ Eq. (B2) demonstrates a “weak attraction” of the dynamics to the nearest state. We also can define in this case a quantity D , which have the meaning of a diffusion coefficient:

$$D(x) = \frac{1}{2} \sum_i p_i(x) \epsilon_i^2. \quad (\text{B5})$$

It is easy to see that in the limit of small δ (assuming $\alpha = \text{const}$) we have:

$$D(x) = \frac{1}{2} \delta^2 + O(\delta^3). \quad (\text{B6})$$

Appendix C: Derivation of the Fokker-Planck equation

We derive the FP equation using the standard integral approach [40]. Namely, we consider an arbitrary function $h(x)$ which has a finite support, that is, localized inside the integration area and is zero together with all of its derivatives for large enough $|x|$. We also assume that it is smooth enough. Then, we write the expression for $\int h(x) \partial_t P(t, x) dx$, assuming integration over the whole real axis:

$$\tau_n \int h(x) \partial_t P(t, x) dx \cong \int h(x) (P(t + \tau_n, x) - P(t, x)) dx, \quad (\text{C1})$$

Expressing $P(t + \tau_n, x)$ through $P(t, x)$ using Eq. (17) and assuming $t = \sum_n \tau_n$, replacing variables in two integral parts as $x \rightarrow x_i(x)$ followed by redefining $x_i \rightarrow x$, and finally expanding $h(x + \epsilon) \cong h(x) + \epsilon h'(x) + \epsilon^2 h''(x)/2$, we transform the later expression into:

$$\int P(t, x) \left(\sum_i p_i (h'(x) \epsilon_i(x) + h''(x) \epsilon_i^2(x)/2) \right) dx. \quad (\text{C2})$$

Applying integration by parts we have finally:

$$\begin{aligned} \int h(x) \{ -\partial_t P(t, x) - \partial_x [\mu(x, t) P(t, x)] + \\ + \partial_{xx} [D(x, t) P(t, x)] \} dx = 0, \end{aligned} \quad (\text{C3})$$

where

$$\mu(x, t) = \sum_i \frac{p_i(x, n) \epsilon_i(x, n)}{\tau_n} \Big|_{n \rightarrow t}, \quad (\text{C4})$$

$$D(x, t) = \sum_i \frac{p_i(x, n) \epsilon_i^2(x, n)}{2\tau_n} \Big|_{n \rightarrow t}. \quad (\text{C5})$$

For small δ and α_n being constant for every n we have, up to the second order of δ :

$$\sum_i p_i(x, t) \epsilon_i(x, t) = \delta_n(x)^2 \tanh(x) + O(\delta_n(x)^3), \quad (\text{C6})$$

$$\sum_i p_i(x, t) \epsilon_i^2(x, t) = \delta_n(x)^2 + O(\delta_n(x)^3). \quad (\text{C7})$$

Taking into account Eq. (24), we finally arrive to Eqs. (26)-(29).

Appendix D: FP coefficients μ and D in different coordinates

We may easily change the variables $x \rightarrow y(x)$ in the FP equation by the known rule [49]:

$$\mu(y) = \mu(x) \partial_x y(x) + D(x) \partial_{xx} y(x), \quad (\text{D1})$$

$$D(y) = D(x) (\partial_x y(x))^2 \quad (\text{D2})$$

In θ -coordinates, given by Eq. (10), we have:

$$\mu(\theta) = -\frac{g^2(\theta) \sin(4\theta)}{8}, \quad D(\theta) = \frac{g^2(\theta) \sin^2(2\theta)}{8}. \quad (\text{D3})$$

For the coordinates $\Pi(x)$ we obtain:

$$\mu(\Pi) = 0, \quad D(\Pi) = 2(\Pi - 1)^2 \Pi^2 g^2(\Pi). \quad (\text{D4})$$

The last equation for $\mu(\Pi)$ reflects the conservation of $\langle \Pi \rangle$ as given by Eq. (19).

-
- [1] Y. S. Patil, S. Chakram, and M. Vengalattore, “Measurement-induced localization of an ultracold lattice gas,” *Phys. Rev. Lett.* **115**, 140402 (2015).
 - [2] M. S. Blok, C. Bonato, M. L. Markham, D. J. Twitchen, V. V. Dobrovitski, and R. Hanson, “Manipulating a qubit through the backaction of sequential partial measurements and real-time feedback,” *Nat Phys* **10**, 189–193 (2014).
 - [3] K. W. Murch, S. J. Weber, C. Macklin, and I. Siddiqi, “Observing single quantum trajectories of a superconducting quantum bit,” *Nature* **502**, 211–214 (2013).
 - [4] M. Hatridge, S. Shankar, M. Mirrahimi, F. Schackert, K. Geerlings, T. Brecht, K. M. Sliwa, B. Abdo, L. Frunzio, S. M. Girvin, R. J. Schoelkopf, and M. H. Devoret, “Quantum back-action of an individual variable-strength measurement,” *Science* **339**, 178–181 (2013).
 - [5] Howard M. Wiseman, “Quantum control: Squinting at quantum systems,” *Nature* **470**, 178–179 (2011).
 - [6] S. Ashhab and Franco Nori, “Control-free control: Manipulating a quantum system using only a limited set of measurements,” *Phys. Rev. A* **82**, 062103 (2010).
 - [7] Christine Guerlin, Julien Bernu, Samuel Deléglise, Clément Sayrin, Sébastien Gleyzes, Stefan Kuhr, Michel Brune, Jean-Michel Raimond, and Serge Haroche, “Progressive field-state collapse and quantum non-demolition photon counting,” *Nature* **448**, 889–893 (2007).
 - [8] Sébastien Gleyzes, Stefan Kuhr, Christine Guerlin, Julien Bernu, Samuel Deleglise, Ulrich Busk Hoff, Michel Brune, Jean-Michel Raimond, and Serge Haroche, “Quantum jumps of light recording the birth and death of a photon in a cavity,” *Nature* **446**, 297–300 (2007).
 - [9] Kater W. Murch, Kevin L. Moore, Subhadeep Gupta, and Dan M. Stamper-Kurn, “Observation of quantum-measurement backaction with an ultracold atomic gas,” *Nat Phys* **4**, 561–564 (2008).
 - [10] Søren Gammelmark, Brian Julsgaard, and Klaus Mølmer, “Past quantum states of a monitored system,” *Phys. Rev. Lett.* **111**, 160401 (2013).
 - [11] Alexander Pechen, Nikolai Il’in, Feng Shuang, and Herschel Rabitz, “Quantum control by von neumann measurements,” *Phys. Rev. A* **74**, 052102 (2006).
 - [12] Goren Gordon, Igor E. Mazets, and Gershon Kurizki, “Quantum particle localization by frequent coherent monitoring,” *Phys. Rev. A* **87**, 052141 (2013).
 - [13] Jonathan B Mackrory, Kurt Jacobs, and Daniel A Steck, “Reflection of a particle from a quantum measurement,” *New Journal of Physics* **12**, 113023 (2010).
 - [14] H.M. Wiseman and G.J. Milburn, *Quantum Measurement and Control* (Cambridge University Press, 2010).
 - [15] Gerardo A. Paz-Silva, A. T. Rezakhani, Jason M. Dominy, and D. A. Lidar, “Zeno effect for quantum computation and control,” *Phys. Rev. Lett.* **108**, 080501 (2012).
 - [16] Carlton M. Caves and G. J. Milburn, “Quantum-mechanical model for continuous position measurements,” *Phys. Rev. A* **36**, 5543–5555 (1987).
 - [17] Ognian Oreshkov and Todd A. Brun, “Weak measurements are universal,” *Phys. Rev. Lett.* **95**, 110409 (2005).
 - [18] Martin Varbanov and Todd A. Brun, “Decomposing generalized measurements into continuous stochastic processes,” *Phys. Rev. A* **76**, 032104 (2007).
 - [19] Yakir Aharonov, David Z. Albert, and Lev Vaidman, “How the result of a measurement of a component of the spin of a spin-1/2 particle can turn out to be 100,” *Phys. Rev. Lett.* **60**, 1351–1354 (1988).
 - [20] Justin Dressel and Andrew N. Jordan, “Weak values are universal in von neumann measurements,” *Phys. Rev. Lett.* **109**, 230402 (2012).
 - [21] Jeff S. Lundeen and Charles Bamber, “Procedure for direct measurement of general quantum states using weak measurement,” *Phys. Rev. Lett.* **108**, 070402 (2012).
 - [22] V.P. Belavkin, “A new wave equation for a continuous nondemolition measurement,” *Physics Letters A* **140**, 355 – 358 (1989).
 - [23] N. Gisin, “Quantum measurements and stochastic processes,” *Phys. Rev. Lett.* **52**, 1657–1660 (1984).
 - [24] H M Wiseman, “Quantum trajectories and quantum measurement theory,” *Quantum and Semiclassical Optics: Journal of the European Optical Society Part B* **8**, 205 (1996).
 - [25] G. G. Gillett, R. B. Dalton, B. P. Lanyon, M. P. Almeida, M. Barbieri, G. J. Pryde, J. L. O’Brien, K. J. Resch, S. D. Bartlett, and A. G. White, “Experimental feedback control of quantum systems using weak measurements,” *Phys. Rev. Lett.* **104**, 080503 (2010).
 - [26] R. I. Karasik and H. M. Wiseman, “How many bits does it take to track an open quantum system?” *Phys. Rev. Lett.* **106**, 020406 (2011).
 - [27] Peter Hänggi and Fabio Marchesoni, “Artificial brownian motors: Controlling transport on the nanoscale,” *Reviews of Modern Physics* **81**, 387 (2009).
 - [28] Peter Reimann, “Brownian motors: noisy transport far from equilibrium,” *Physics Reports* **361**, 57 – 265 (2002).
 - [29] O.M. Braun and Y.S. Kivshar, *The Frenkel-Kontorova Model: Concepts, Methods, and Applications* (Physics and Astronomy Online Library (Springer, 2004).
 - [30] Degang Wu and Kwok Yip Szeto, “Extended Parrondo’s game and Brownian ratchets: Strong and weak Parrondo effect,” *Phys. Rev. E* **89**, 022142 (2014).
 - [31] M Velez, JI Martin, JE Villegas, Axel Hoffmann, EM González, JL Vicent, and Ivan K Schuller, “Superconducting vortex pinning with artificial magnetic nanostructures,” *Journal of Magnetism and Magnetic Materials* **320**, 2547–2562 (2008).

- [32] Clécio C de Souza Silva, Joris Van de Vondel, Mathieu Morelle, and Victor V Moshchalkov, “Controlled multiple reversals of a ratchet effect,” *Nature* **440**, 651–654 (2006).
- [33] JE Villegas, EM Gonzalez, MP Gonzalez, José Virgilio Anguita, and JL Vicent, “Experimental ratchet effect in superconducting films with periodic arrays of asymmetric potentials,” *Physical Review B* **71**, 024519 (2005).
- [34] J. M. R. Parrondo, “How to cheat a bad mathematician,” in *EEC HC&M Network on Complexity and Chaos* (ISI, Torino, Italy, 1996).
- [35] Andrew Allison and Derek Abbott, “The physical basis for Parrondo’s games,” *Fluctuation and Noise Letters* **2**, L327–L341 (2002).
- [36] Łukasz Paweł and Jan Ślaskowski, “Cooperative quantum Parrondos games,” *Physica D: Nonlinear Phenomena* **256**, 51–57 (2013).
- [37] C.M. Chandrashekar and Subhashish Banerjee, “Parrondos game using a discrete-time quantum walk,” *Physics Letters A* **375**, 1553 – 1558 (2011).
- [38] David Bulger, James Freckleton, and Jason Twamley, “Position-dependent and cooperative quantum Parrondo walks,” *New Journal of Physics* **10**, 093014 (2008).
- [39] A.P. Flitney, J. Ng, and D. Abbott, “Quantum Parrondo’s games,” *Physica A: Statistical Mechanics and its Applications* **314**, 35 – 42 (2002).
- [40] Crispin W Gardiner and C Gardiner, *Stochastic methods: a handbook for the natural and social sciences* (World Publishing Corporation, 1984).
- [41] T. A. Brun, “A simple model of quantum trajectories,” *American Journal of Physics* **70**, 719–737 (2002), arXiv:quant-ph/0108132.
- [42] Michel Bauer, Tristan Benoist, and Denis Bernard, “Repeated quantum non-demolition measurements: Convergence and continuous time limit,” in *Annales Henri Poincaré* (Springer, 2013) pp. 1–41.
- [43] Charles R. Doering, “Stochastic ratchets,” *Physica A: Statistical Mechanics and its Applications* **254**, 1 – 6 (1998).
- [44] Rolf H Luchsinger, “Transport in nonequilibrium systems with position-dependent mobility,” *Physical Review E* **62**, 272 (2000).
- [45] P Lançon, G Batrouni, L Lobry, and N Ostrowsky, “Drift without flux: Brownian walker with a space-dependent diffusion coefficient,” *EPL (Europhysics Letters)* **54**, 28 (2001).
- [46] R Krishnan, Surjit Singh, and GW Robinson, “Space-dependent friction in the theory of activated rate processes,” *Physical Review A* **45**, 5408 (1992).
- [47] NG Van Kampen, “Relative stability in nonuniform temperature,” *IBM Journal of Research and Development* **32**, 107–111 (1988).
- [48] Rolf Landauer, “Motion out of noisy states,” *Journal of Statistical Physics* **53**, 233–248 (1988).
- [49] H. Risken, *The Fokker-Planck Equation: Methods of Solution and Applications* (World Publishing Corporation, 1984).